Dehydrogenation of Perhydro-N-ethylcarbazole Under Reduced Total Pressure

Stephan Kiermaier[a], Daniel Lehmann[a], Andreas Bösmann[a], Peter Wasserscheid[a,b]*

[a] Lehrstuhl für Chemische Reaktionstechnik, Friedrich-Alexander-Universität Erlangen-Nürnberg (FAU), Egerlandstr. 3, D-91058, Erlangen, Germany

[b] Helmholtz-Institute Erlangen-Nürnberg for Renewable Energies, IEK-11, Forschungszentrum Jülich, Nägelsbachstraße 59, 91058 Erlangen, Germany

* Corresponding author. E-mail: peter.wasserscheid@fau.de

Abstract

Liquid organic hydrogen carrier (LOHC) systems represent a promising storage option for hydrogen produced from renewable electricity by water electrolysis. Regarding the efficiency of the endothermal hydrogen release reaction, this technology greatly benefits from a direct heat integration with the waste heat of the energetic use of the released hydrogen, e. g. in a fuel cell. To enable such beneficial set-up, the reaction temperature of hydrogen release must be below the operation temperature of the applied fuel cell which calls for both low temperature dehydrogenation catalysis and high temperature fuel cell operation. This paper demonstrates that such combination may be suitable if reduced pressure dehydrogenation of perhydro-N-ethylcarbazole (H12-NEC) is combined with hydrogen electrification in a high temperature polymer electrolyte membrane fuel cell (HT-PEMFC). Dehydrogenation reactions of H12-NEC were carried out between 160 °C and 200 °C applying different hydrogen partial pressures in the dehydrogenation unit to mimic the effect of a sucking fuel cell operation mode, i.e. the reduction of hydrogen partial pressure in the dehydrogenation unit caused by the fuel cell operation. Our kinetic analysis reveals that a dehydrogenation temperature of 180 °C combined with 500 mbar hydrogen partial pressure represent, for example, a suitable parameter set for efficient hydrogen release.

Keywords: LOHC, N-ethylcarbazole, dehydrogenation, hydrogen partial pressure, fuel cell

Introduction

Liquid organic hydrogen carriers (LOHCs) offer an attractive option to store intermittent renewable energies from wind and solar power units in the form of chemically bound hydrogen [1]. In future clean energy scenarios these carriers can be charged with hydrogen at energy-rich times and windy/sunny locations by catalytic hydrogenation. The so-obtained hydrogen-rich form of the LOHC system can be stored and transported in a safe and energy-dense form [2]. Due to their liquid nature, LOHC systems hold the promise that they can be distributed via the existing infrastructure for fossil fuels [3]. At the place and time of energy demand, the hydrogen stored in the hydrogen-rich form of the LOHC system can be released by a catalytic dehydrogenation reaction, while the discharged LOHC system is ready for another round of the hydrogen storage cycle [2, 4]. The main driving force for this storage cycle that resembles the filling and emptying of a refundable bottle (here the liquid organic carrier) with a valuable content (here the green hydrogen) is the applied hydrogen partial pressure. While the hydrogenation step takes place at the elevated pressures of the electrolyser hydrogen output stream (typically above 15 bar hydrogen partial pressure), the dehydrogenation step proceeds at significantly lower hydrogen partial pressure, typically below 5 bar [5].

Like in all other power-to-liquid technologies [6], the hydrogen charging process of the LOHC cycle, i.e. the catalytic hydrogenation step, is exothermal. In contrast, hydrogen release, i.e. the catalytic dehydrogenation of the charged liquid carrier, is endothermal. Because in most application scenarios the released hydrogen is utilized immediately (this is the reason why hydrogen release takes place), the heat demand of the hydrogen release step and the waste heat production in the hydrogen utilization step can be coupled. Such heat integration can strongly increase the energetic efficiency of the hydrogen release from LOHC systems [7]. If, for example, a fuel cell is applied to reconvert the released hydrogen to produce electricity, about 50 % of the energy is released as waste heat [8]. Thus, a proper heat integration between the exothermic fuel cell reaction and the endothermic dehydrogenation is highly desirable [9, 10].

Müller *et al.* highlighted that using the excess heat from a fuel cell to carry out the dehydrogenation is the optimal configuration for hydrogen release from LOHC systems with respect to energy efficiency [11]. This option was proposed early on in LOHC research, however, traditional approaches using low temperature PEM fuel cells are characterized by a temperature mismatch between the operating temperatures of the LOHC dehydrogenation and the temperature level of the fuel cell operation [2, 3]. Note, that the temperature level of the

exothermal fuel cell operation should be at least 20 °C higher than the temperature level of the dehydrogenation reaction to enable effective heat transfer and heat integration.

The present study builds on the current progress in high temperature PEM fuel technologies based on phosphoric acid-doped polybenzimidazole (PBI) membranes [12]. Besides other interesting features like their high tolerance to impurities and increased electrode kinetics due to the high operating temperature HT-PEM modules enable stable long-term performance at temperatures of 160 - 200 °C [12-17]. This defines the technical task to operate LOHC dehydrogenation at high rates and excellent selectivity (i.e. no formation of products that are not intermediates or products of the storage cycle) in the temperature range between 140 °C and 180 °C.

Amongst today's most relevant LOHC-systems, some tend to be more capable of a dehydrogenation at low temperatures than others [18]. Generally, the energy demand to release hydrogen from LOHCs is largely dependent on the heat capacity and on the reaction enthalpy of the system [19]. As the reaction enthalpy also determines the temperature-level of the dehydrogenation reaction, desirable values were set to 42 - 54 kJ*mol$^{-1}_{H_2}$ by Cooper *et al.* [20] and 40 – 70 kJ*mol$^{-1}_{H_2}$ by Wild *et al.* [21] to enable hydrogen-release at moderate conditions [22]. The most prominent examples of LOHC-systems like toluene / methylcyclohexane (71.8 kJ*mol$^{-1}_{H_2}$ [23]), dibenzyltoluoene / perhydro-dibenzyltoluene (65.4 kJ*mol$^{-1}_{H_2}$ [19]) benzyltoluene / perhydrobenzyltoluene (63.5 kJ*mol$^{-1}_{H_2}$ [19, 24]), and N-ethylcarbazole (H0-NEC) / perhydro-N-ethylcarbazole (H12-NEC) (43.2 kJ*mol$^{-1}_{H_2}$ [25-27]) have been examined in detail regarding these thermophysical and thermochemical properties. LOHC systems with particularly favorable thermodynamics for hydrogen release are heterocyclic compounds, especially 5-membered ring systems, such as the H0-NEC/H12-NEC system [28, 29]. The reaction scheme and typically applied reaction conditions for this LOHC system are depicted in figure 1.

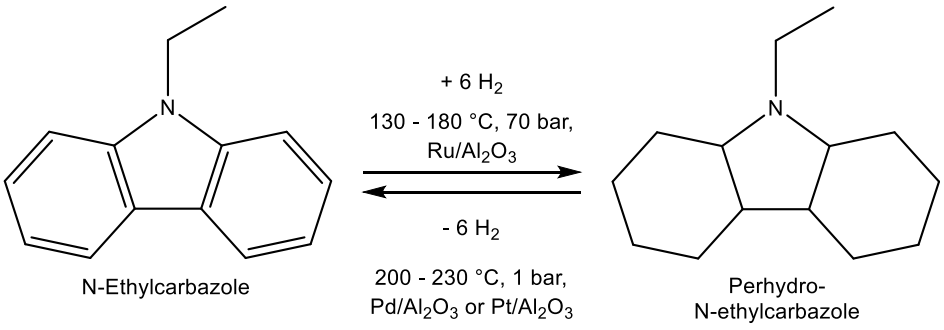

Figure 1: Chemical hydrogen storage using the N-ethylcarbazole (NEC)/ perhydro-N-ethylcarbazole (H12-NEC) LOHC system - typically applied hydrogenation and dehydrogenation catalysts and reaction conditions [2, 30-32].

The use of H0-NEC/H12-NEC as hydrogen storage system was proposed by Pez *et al.* from Air Products and Chemicals in 2006 [33]. Despite of many alternative LOHC systems under investigation - some showing better technical availability, better stability, slightly higher storage capacity and more suitable ecotoxicology – the NEC / H12-NEC system still counts amongst the most interesting LOHC candidates [10, 34]. The fully loaded form, H12-NEC, has a hydrogen capacity of 5.8 wt. %, which meets the 2020 and 2025 U.S. Department of Energy's (DOE) technical performance targets for hydrogen storage systems for onboard light-duty vehicles [35].

The relatively low enthalpy of dehydrogenation for H12-NEC enables efficient hydrogen release at comparably mild reaction conditions, e.g. at temperatures below 200 °C [10]. The hydrogenation of NEC for hydrogen storage is usually carried out at 130 - 180 °C and pressures up to 70 bar over supported noble metal catalysts [31, 36-40]. The obtained isomers were analyzed via GC-MS, 1D- and 2D-NMR techniques by Eblagon *et al.* [31]. These authors postulated the formation of 16 H12-NEC stereoisomers, of which six molecules are distinguishable by NMR.

The heterogeneously catalyzed dehydrogenation of H12-NEC for hydrogen release has been investigated using Pt-[34, 41-43], Pd-[29, 32, 34, 36, 37, 42, 44, 45], Ru-[42] and Rh-based[42] catalysts. The focus of current LOHC research is typically on the dehydrogenation reaction, as this reaction is more challenging than LOHC hydrogenation due to the endothermic character of the reaction [46]. The biggest challenge during the dehydrogenation of H12-NEC is to avoid the formation of an unwanted side-products that form by the cleavage of the C-N bond in the molecule and that lead to partly hydrogenated carbazole by-products [32, 34, 37]. It has been shown that an effective production of hydrogen from H12-NEC is possible at 200 - 230 °C and pressures slightly above ambient conditions [2]. Generally, as one would expect, a higher temperature has been found to result in higher hydrogen release rates [34, 36]. Note, that a direct comparison of the H12-NEC dehydrogenation studies in the literature is difficult. Often, the authors apply carrier gas or use a volatile solvent, measures that reduce the hydrogen partial pressure in the reactor in a typically not very well defined manner [29, 36, 42, 44, 45]. More importantly, these measures either dilute the reaction system or add an unwanted contamination to the released hydrogen.

This paper reports on low-temperature perhydro-N-ethylcarbazole dehydrogenation to open the path for proper heat integration between a high temperature PEM fuel cell and H12-NEC-based hydrogen storage. To the best of our knowledge this is the first report on enhancing hydrogen

release from H12-NEC by reducing the total pressure of the dehydrogenation system. Our paper focuses on the interplay of different pressure and temperature levels to enable optimized dehydrogenation productivities at temperatures below 200 °C using commercial Pd/alumina and Pd/C catalysts. Kinetic investigations and by-product analysis are carried out to gain further information on the technical applicability of H12-NEC dehydrogenation at pressures below ambient.

Experimental

Materials

Perhydro-N-ethylcarbazole (H12-NEC) was synthesized in a Parr autoclave (Model 4568). Prior to hydrogenation, 146 g of N-ethylcarbazole (H0-NEC, Alfa Aesar, 99 % purity) were weighed into the reactor. As catalysts, 1.52 g of Ru/alumina (Aldrich, Lot: X12E020; 5 wt. % powder, molar ratio $n_{Ru} : n_{H0\text{-}NEC} = 1 : 1000$) and 0.80 g Pd/alumina (Aldrich, batch: 10221PE; 5 wt. % powder, molar ratio $n_{Pd} : n_{H0\text{-}NEC} = 1 : 2000$) were added. The reactor was sealed and purged with argon (Air Liquide, 99.998 %). After heating to the desired reaction temperature (T = 160 °C), hydrogen (Linde 99.999 %) was added (p = 40 bar) and the stirrer was set to 1200 rpm to start gas entrainment. The reaction was carried out for at least 72 h to guarantee full hydrogenation. After cooling down, the formed H12-NEC was filtered to remove the catalyst from the hydrogen-charged carrier liquid. Wherever possible, the liquid was handled under argon to avoid unwanted reactions with oxygen from ambient air. As elemental analysis of the hydrogenated LOHC still showed some impurities of sulfur (970 – 2380 ppmw) from the supplied feedstock quality, the obtained H12-NEC was stirred at room temperature over night with a heterogeneous Pt/alumina catalyst (Alfa Aesar, Lot: H30X002; 1 wt. %, 2.7 - 3.3 mm spheres, molar ratio $n_{Pt} : n_{H12\text{-}NEC} \approx 1 : 1500$) to guarantee removal of all remaining S-compounds. In this way, we reached reproducibly a S-free standard quality of H12-NEC for our dehydrogenation experiments. The sulfur-content was checked for each batch of H12-NEC and was found in all cases to be below the detection limit of 200 ppmw.

GC analysis resolved a total number of five different perhydro-N-ethylcarbazole species of which three were only detectable in small amounts. In an earlier study, Eblagon *et al.* also found two main H12-NEC species via GC-MS analysis after H0-NEC hydrogenation [31]. The composition of the different stereoisomers that were distinguishable via GC-MS was the same

for all H12-NEC batches produced. Further species that were identified via GC-MS are octahydro-N-ethylcarbazole (H8-NEC), hexahydro-N-ethylcarbazole (H6-NEC), tetrahydro-N-ethylcarbazole (H4-NEC) and dihydro-N-ethylcarbazole (H2-NEC), and N-ethylcarbazole (H0-NEC). H2-NEC was only found in traces in some liquid samples. As by-products, GC-MS analysis revealed species that arose from the cleavage of the C-N bond of the molecule. We identified perhydro-carbazole (H12-C), decahydro-carbazole (H10-C), octahydro-carbazole (H8-C) tetrahydrocarbazole (H4-C), and also fully unloaded carbazole (H0-C). The detailed composition of a typical product mixture obtained from H0-NEC hydrogenation is given in the Supporting Information.

All dehydrogenation reactions in the present study were carried out with commercial catalysts, namely Pd/alumina (Aldrich, batch: 10221PE; 5 wt. % powder) and Pd/carbon (Aldrich, Lot: MKBS9242V; 5 wt. % powder). Characterization data of the applied catalysts (BET surface, Pd-content, dispersion) were determined and can be found in the Supporting Information.

Setup for H12-NEC dehydrogenation

Our dehydrogenation experiments were carried out in a 100 ml three-neck flask with an intensive condenser attached to it. The glass reactor was equipped with a heating jacket and a magnetic stirrer. The H12-NEC was filled into the reactor together with the catalyst and purged with argon to remove air. During the experiment, no solvents or inert gas streams were used in the reactor to avoid falsification of the obtained kinetic data by manipulation of the hydrogen partial pressure in the reactor. The starting point of the dehydrogenation reactions was defined at the moment where the desired reaction temperature was reached. At the same time, the system pressure was adjusted via a Venturi nozzle. Nitrogen was used as operating medium in the nozzle to avoid the generation of flammable gas mixtures. Fine regulation of the system pressure was carried out by adjusting the nitrogen flow with a pressure regulator and a needle valve. Temperature and system pressure were monitored continuously throughout the whole experiment. Liquid samples were taken at fixed times with a syringe. The catalyst powder was filtered off with a PTFE syringe filter before liquid sample analysis was performed.

Analysis

Analysis of the sulfur contaminations was carried out via elemental analysis. The applied Elementar Unicube was equipped with a thermal conductivity detector and an IR detector to

measure trace amounts of sulfur. The different N-ethylcarbazole species were analyzed with a Bruker Scion GC-MS equipped with a Restek Rtx-225 30 m x 0.25 µm capillary column and a single quadrupole mass analyzer. The reaction progress of the experiments was monitored via gas chromatography. The Varian 3900 GC used was equipped with a Restek Rtx-225 30 m x 0.25 µm capillary column and a flame ionization detector. Catalyst support characterization was carried out by N_2-physisorption with a Quadrasorb SI from the company Quantachrome Instruments. The supported catalytic noble metal nanoparticles were investigated via CO-chemisorption with an Autochem II 2920 from Micromeritics.

Results

The upper limit of the dehydrogenation temperatures applied in this study was 200 °C as this was regarded as the highest realistic temperature for using waste heat from a HT-PEM fuel cell as heat source for the LOHC dehydrogenation. The lower limit of the dehydrogenation temperatures for our experiment was 160 °C for thermodynamic and kinetic reasons. Our experiments were carried out at different pressure levels to quantify the expected accelerating effect of a lower system pressure on the dehydrogenation reaction.

The degree of dehydrogenation (DoDH) as a measure for the amount of hydrogen released at a certain time in comparison to the maximum amount of hydrogen that can be stored was determined via equation 1

$$DoDH(t) = 1 - \frac{n_{H_2,LOHC}(t)}{n_{H_2,LOHC,max}} \qquad \text{Equation 1}$$

Dehydrogenation at 200 °C with Pd/alumina *vs.* Pd/carbon

Our first set of dehydrogenation experiments was carried out using Pd on alumina at 200 °C. The experiments were performed at atmospheric pressure, 500 mbar and 250 mbar total pressure. Even at a pressure of p = 250 mbar, the evaporation of the LOHC and the observable reflux from the condenser was found to be low. H12-NEC is therefore well suited for dehydrogenation experiments below atmospheric pressure.

From the GC product analyses the degree of dehydrogenation (*DoDH*) as a measure of the released hydrogen were determined. The *DoDHs* and the molar fractions of the various Hx-NEC components are shown are in figure 2.

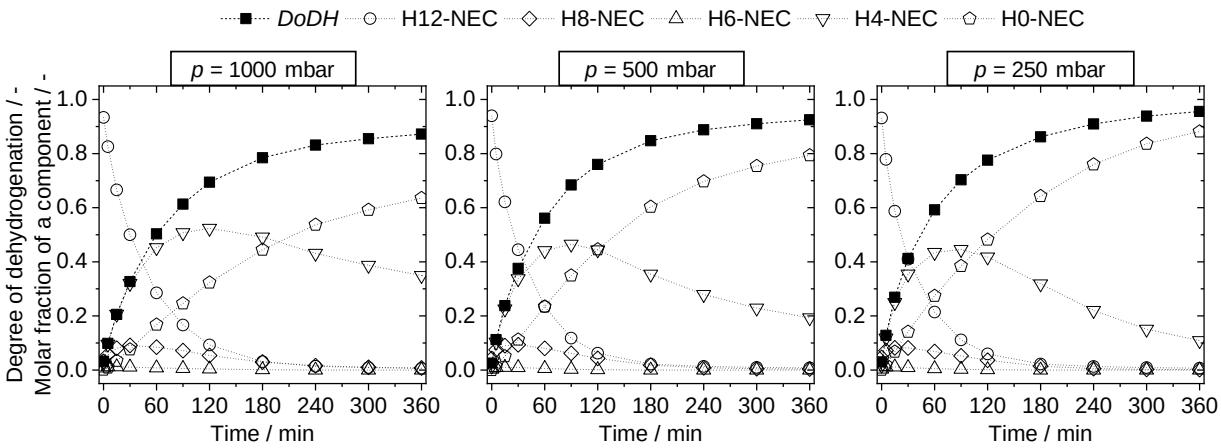

Figure 2: Degree of dehydrogenation and molar fraction of the different Hx-NEC components as function of time at 200 °C and 1000 mbar (left), 500 mbar (middle), and 250 mbar (right), respectively.
Experimental conditions: T = 200 °C, $n_{\mathrm{H12\text{-}NEC,0}}$ = 0.05 mol, $n_{\mathrm{Pd}} : n_{\mathrm{H12\text{-}NEC}}$ = 1 : 1000; catalyst: Pd/alumina 5 wt. %.

All three experiments show rapid dehydrogenation of H12-NEC. Amongst the different intermediate species, H8-NEC forms first, and later H4-NEC becomes a major compound in the mixture. The intermediate H6-NEC is only detected in very small amounts mostly in the first hour of the reaction. The final product of dehydrogenation, H0-NEC, is formed at last in the dehydrogenation sequence. In all three experiments, the accumulation of H4-NEC is most pronounced which hints for the fact that the dehydrogenation of this compound is the rate determining step for the whole reaction progress. The final *DoDH* after 6 h slightly increases with reducing the total pressures (87.2 % at p = 1000 mbar, 92.5 % at p = 500 mbar and 95.5 % at p = 250 mbar). Apparently, the dehydrogenation rate is affected by the hydrogen partial pressure (and thus by the total pressure) in the dehydrogenation reactor. At lower pressures, the thermodynamic equilibrium is shifted to the side of the dehydrogenated products resulting in an increased driving force for the dehydrogenation process.

For our experiments with the commercial Pd on carbon catalyst the metal loading was kept constant and the Pd dispersion was in the same range on both supports (see Supporting Information for details). The *DoDHs* and the composition of the reaction mixture over time at 200 °C with this catalyst are presented in figure 3. The carbon-based Pd catalyst shows a faster dehydrogenation compared to the previous experiments using Pd on alumina at 200 °C as indicated by the higher *DoDHs* after 6 h (90.1 % at p = 1000 mbar, 95.9 % at p = 500 mbar and

99.0 % at p = 250 mbar). Again, H8-NEC and H4-NEC were found as the main intermediates. The promising results with carbon-based catalysts should motivate further research on the performance and stability of these catalyst materials under process conditions.

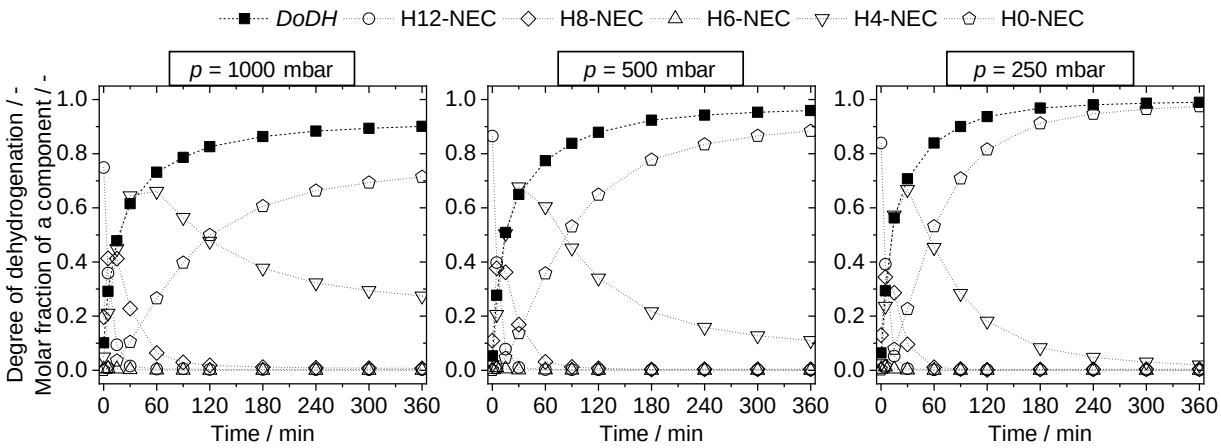

Figure 3: Degree of dehydrogenation and molar fraction of the different Hx-NEC components as a function of time at 200 °C at 1000 mbar (left), 500 mbar (middle) and 250 mbar (right)
Experimental conditions: T = 200 °C, $n_{\text{H12-NEC,0}}$ = 0.05 mol, n_{Pd} : $n_{\text{H12-NEC}}$ = 1 : 1000; catalyst: Pd/carbon 5 wt. %.

Dehydrogenation at 180 °C with Pd/alumina *vs.* Pd/carbon

In the next set of experiments, the H12-NEC dehydrogenation was investigated with both catalyst at 180 °C. Figure 4 shows the *DoDHs* and the composition of the reaction mixture as a function of time for the three pressure levels of 1000 mbar, 500 mbar, and 250 mbar with the Pd/alumina catalyst.

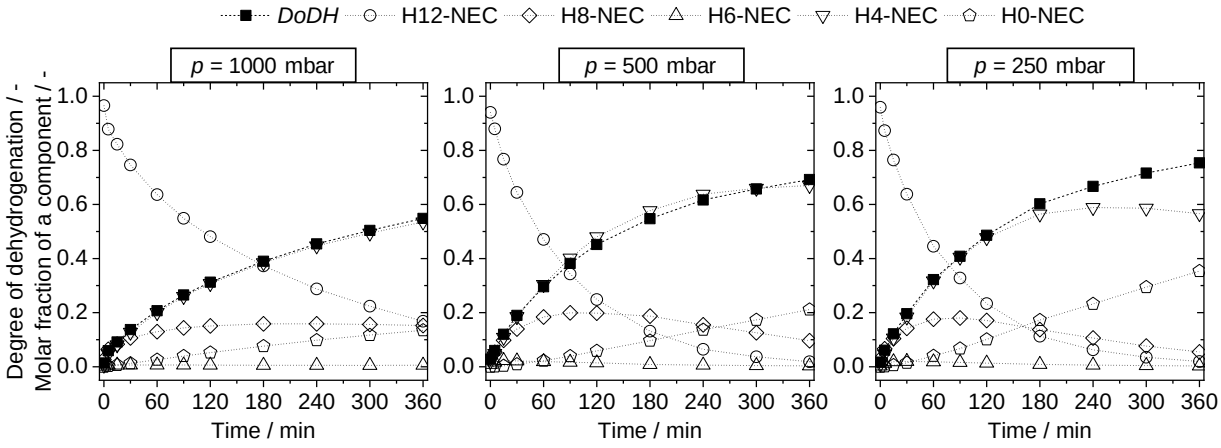

Figure 4: Degree of dehydrogenation and molar fraction of the different Hx-NEC components as a function of time at 180 °C at 1000 mbar (left), 500 mbar (middle) and 250 mbar (right), respectively.
Experimental conditions: T = 180 °C, $n_{\text{H12-NEC,0}}$ = 0.05 mol, n_{Pd} : $n_{\text{H12-NEC}}$ = 1 : 1000; catalyst: Pd/alumina 5 wt. %.

As expected, the dehydrogenation rate is significantly lower at 180 °C compared to 200 °C with the same catalyst. The degree of dehydrogenations still reaches significant levels after 360 min reaction time (54.8 % at p = 1000 mbar, 69.2 % at p = 500 mbar and 75.4 % at p = 250 mbar). The intermediate H8-NEC is present during the whole reaction time, whereas H4-NEC accumulates strongly. The formation of the fully dehydrogenated product, H0-NEC, is strongly pressure dependent. In more general, the pressure influence on *DoDH* seems to be stronger for the H12-NEC dehydrogenation at 180 °C compared to 200 °C.

Also the carbon-supported Pd catalyst was tested at 1000 mbar, 500 mbar and 250 mbar total pressure at 180 °C. Figure 5 depicts the *DoDHs* and the respective compositions of the reaction mixtures over time.

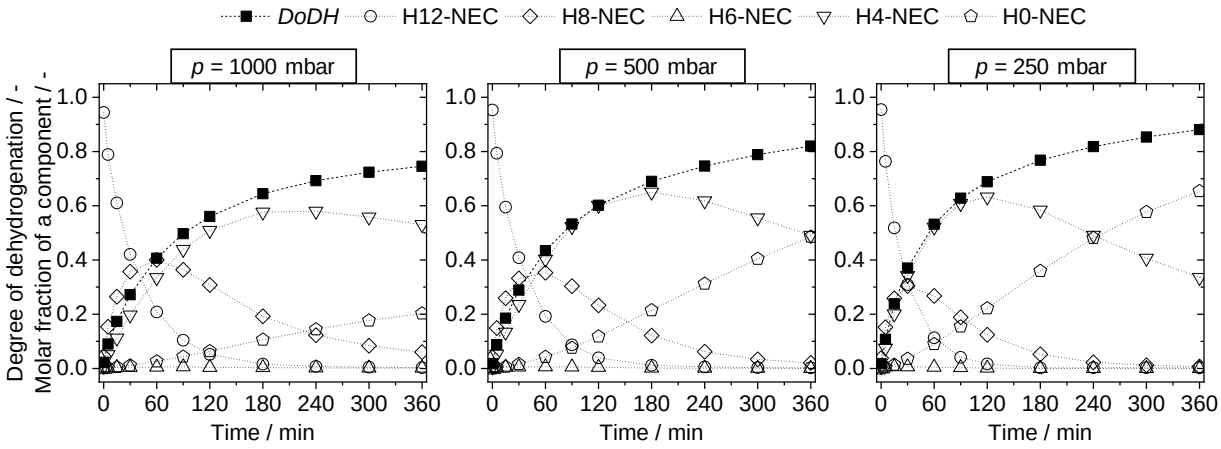

Figure 5: Degree of dehydrogenation and molar fraction of the different Hx-NEC components as a function of time at 180 °C at 1000 mbar (left), 500 mbar (middle) and 250 mbar (right)
Experimental conditions: T = 180 °C, $n_{H12\text{-}NEC,0}$ = 0.05 mol, n_{Pd} : $n_{H12\text{-}NEC}$ = 1 : 1000; catalyst: Pd/carbon 5 wt. %.

Again, the dehydrogenation reaction proceeds faster with the carbon-based catalyst system compared to the Pd/alumina system. The final *DoDHs* after 6 h (74.6 % at p = 1000 mbar, 82.0 % at p = 500 mbar and 88.1 % at p = 250 mbar) were far above the values that were reached at 180 °C with the alumina supported catalyst. The main intermediates H8-NEC and H4-NEC both show maxima depending on the pressure level between 30 and 60 minutes and 120 and 180 minutes, respectively. The formation of the last intermediate of the dehydrogenation sequence, namely H0-NEC, shows again a strong pressure dependence.

Dehydrogenation at 160 °C with Pd/alumina *vs.* Pd/carbon

Finally, another set of comparative experiments was carried out at a temperature of 160 °C. Figure 6 presents the *DoDHs* and the molar fractions as a function of time at the three different pressure levels with the Pd/alumina catalyst.

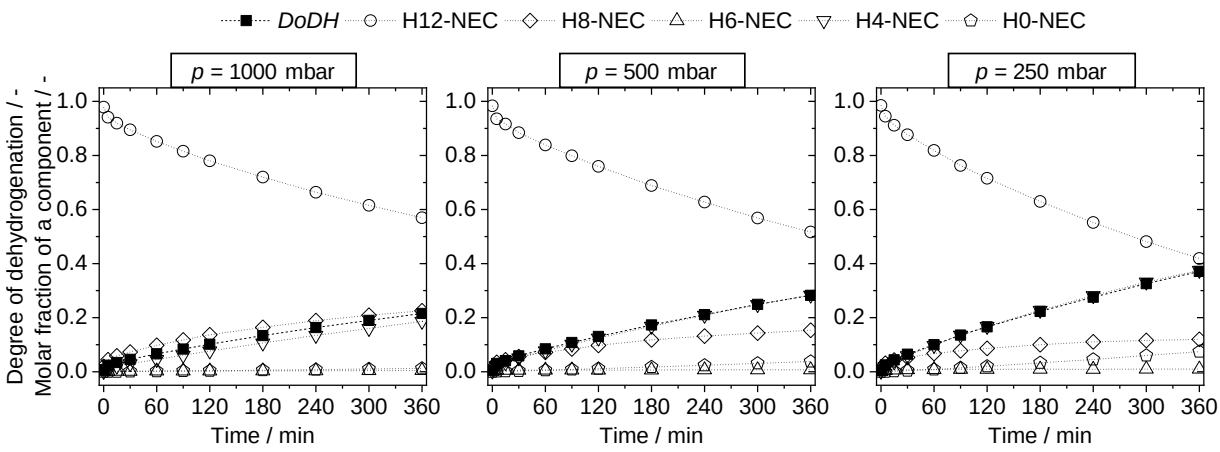

Figure 6: Degree of dehydrogenation and molar fraction of the different Hx-NEC components as a function of time at a temperature of 160 °C at 1000 mbar (left), 500 mbar (middle) and 250 mbar (right), respectively.
Experimental conditions: T = 160 °C, $n_{\text{H12-NEC,0}}$ = 0.05 mol, n_{Pd} : $n_{\text{H12-NEC}}$ = 1 : 1000; catalyst: Pd/alumina 5 wt. %.

At 160 °C the reaction is slower but hydrogen release is still notable after 360 min (*DoDHs* of 21.5 % at p = 1000 mbar, 28.3 % at p = 500 mbar and 37.1 % at p = 250 mbar), with 73 % higher *DoDH* at 250 mbar compared to ambient pressure. Again, the two species H8-NEC and H4-NEC are formed as most abundant intermediates. The results with the Pd/carbon catalyst at 160 °C are shown in figure 7.

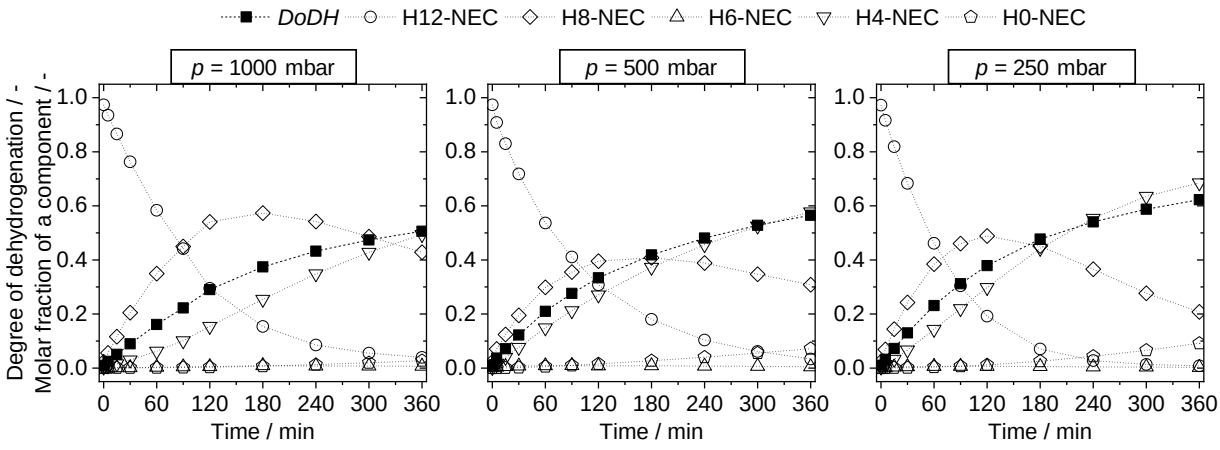

Figure 7: Degree of dehydrogenation and molar fraction of the different Hx-NEC components as a function of time at 160 °C at 1000 mbar (left), 500 mbar (middle) and 250 mbar (right)
Experimental conditions: T = 160 °C, $n_{\text{H12-NEC,0}}$ = 0.05 mol, n_{Pd} : $n_{\text{H12-NEC}}$ = 1 : 1000; catalyst: Pd/carbon 5 wt. %.

Also at this relatively low temperature, the Pd/carbon catalyst outperforms the alumina-supported system. The hydrogen release after 6 h is higher with this catalyst at all applied pressure levels (50.6 % at p = 1000 mbar, 56.5 % at p = 500 mbar and 62.3 % at p = 250 mbar), the relative pressure influence seems to be smaller. While the reaction rates at 160 °C are lower compared to the experiments at higher temperatures, it can be shown that H12-NEC dehydrogenation is quite effective at temperatures as low as 160 °C, in particular at reduced total pressure and with the carbon supported Pd catalyst. Even faster hydrogen release would be possible by applying a higher catalyst to H12-NEC ratio.

Productivities in H12-NEC dehydrogenation at various total pressures

Depending on the application under consideration, a quick hydrogen release from the charged LOHC system is required, while in other cases a steady and slow dehydrogenation is sufficient. The experiments shown above were therefore evaluated from a kinetic point of view to get a quantitative measure of the hydrogen productivity in terms of mass hydrogen produced per mass Pd and time [unit: $g(H_2)/(g(Pd) \cdot min)$]. The productivity information allows for a proper comparison of the different operating points under investigation in this study. Next to the catalytic productivities, the rate constants k of H12-NEC consumption were determined and can be found in the Supporting Information. Activation energies of this first step of H12-NEC dehydrogenation were found to be between 91.9 and 100.6 kJ/mol for the alumina-based system and between 69.4 and 81.7 kJ/mol for the Pd/carbon catalyst (see Supporting Information). A comparison of the productivities determined within the first 2 h reaction time for the alumina-based Pd catalyst system is found in figure 8.

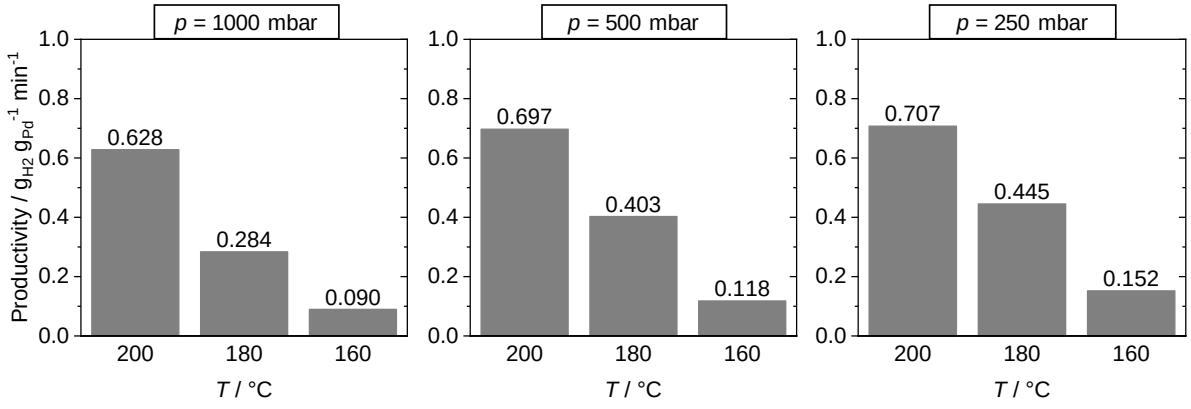

Figure 8: Overall productivities of the dehydrogenation reactions of H12-NEC at the temperature levels of 200 °C, 180 °C and 160 °C and at pressures of 1000 mbar (left), 500 mbar (middle) and 250 mbar (right) after 2 h
Experimental conditions: $n_{H12\text{-}NEC,0}$ = 0.05 mol, n_{Pd} : $n_{H12\text{-}NEC}$ = 1 : 1000; catalyst: Pd/alumina 5 wt. %.

As expected from the Arrhenius law, the highest productivities are found for a temperature of 200 °C. It is remarkable, however, that at 180 °C under 500 mbar and 250 mbar total pressure, 60% of the productivity values of the experiments at 200 °C at ambient pressure are reached.

The same productivity analysis was carried out for the carbon-based Pd catalyst and is presented in figure 9.

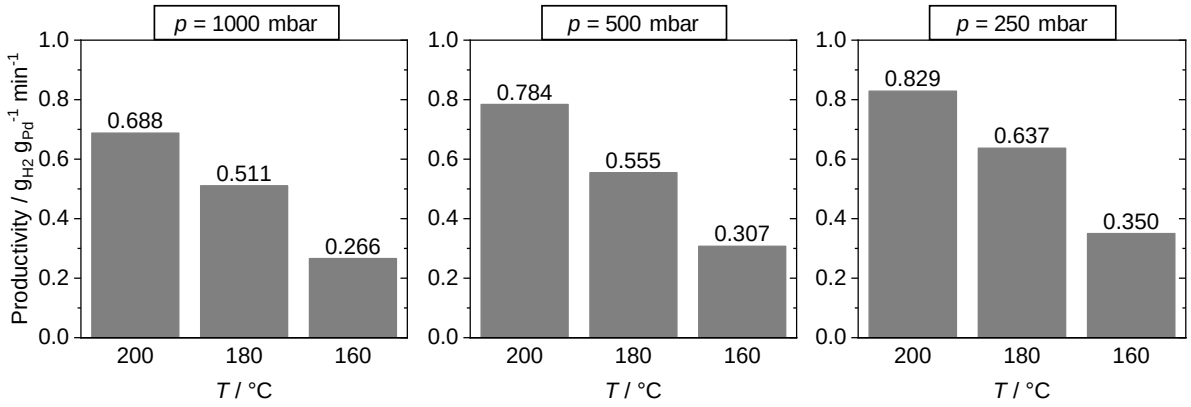

Figure 9: Overall productivities of the dehydrogenation reactions of H12-NEC at the temperature levels of 200 °C, 180 °C and 160 °C and at pressures of 1000 mbar (left), 500 mbar (middle) and 250 mbar (right) after 2 h
Experimental conditions: $n_{H12\text{-}NEC,0}$ = 0.05 mol, n_{Pd} : $n_{H12\text{-}NEC}$ = 1 : 1000; catalyst: Pd/carbon 5 wt. %.

Again, the highest productivities were found at a temperature of 200 °C. At 180 °C the productivity of the Pd/carbon catalyst at 250 mbar is close to the value that was obtained at atmospheric conditions at 200 °C. In comparison to the alumina-based catalyst system the productivities were higher with the Pd/carbon catalyst at all operating points. Very interestingly, the decrease in productivity by lowering the temperature from 180 °C to 160 °C is less pronounced with the Pd/carbon catalyst. We therefore conclude that the carbon-based Pd catalyst is most suitable for H12-NEC dehydrogenation at mild conditions. This should motivate future catalyst optimization studies for low-temperature H12-NEC dehydrogenation based on carbon supported precious metal catalyst systems.

Byproduct formation during dehydrogenation reaction

When discussing the technical applicability of a LOHC hydrogen storage system multiple excellent recyclability of the LOHC storage medium is mandatory. The N-ethylcarbazole-based LOHC system is known for its tendency for byproduct formation in the dehydrogenation reaction via cleavage of its C-N bond. This undesired reaction leads to the formation of different carbazole species. In principle, these molecules can function as LOHC molecules as well. They

display, however, different physico-chemical properties, such as higher melting points and higher viscosity in the molten state.

Initially, we considered three possible influencing factors that should affect the tendency for C-N bond cleavage in NEC-based LOHC compounds, namely i) the reaction temperature, ii) the reaction pressure, and iii) the nature of the applied catalyst. In this study, two different catalyst materials, three different temperatures and three different pressures have been applied to allow conclusions on the relative relevance of these influencing factors. Table 1 gives the sum of all detected Hx-carbazole species in the reaction mixture for experiments with Pd on alumina after 1 h, 2 h and 6 h reaction time, respectively.

Table 1: Sum of the molar fractions of all emerging Hx-carbazole by-products in the dehydrogenation reactions of H12-NEC at 200 °C, 180 °C, 160 °C at the pressure levels of 1000 mbar, 500 mbar and 250 mbar after 1 h / 2h / 6 h reaction time.

	***p* = 1000 mbar**	***p* = 500 mbar**	***p* = 250 mbar**
***T* = 200 °C**	0.7 % / 0.8 % / 2.4 %	1.0 % / 1.2 % / 3.1 %	0.9 % / 1.5 % / 3.6 %
***T* = 180 °C**	0.8 % / 0.9 % / 1.4 %	1.4 % / 1.9 % / 2.8 %	2.0 % / 2.8 % / 4.3 %
***T* = 160 °C**	0.4 % / 0.6 % / 1.0 %	0.4 % / 0.5 % / 0.6 %	0.4 % / 0.7 % / 1.2 %

Experimental conditions: $n_{H12\text{-}NEC,0}$ = 0.05 mol, n_{Pd} : $n_{H12\text{-}NEC}$ = 1 : 1000; catalyst: Pd/alumina 5 wt. %.

As expected, higher reaction temperature and lower total pressure promote the dealkylation reaction. In addition, the data indicate that the aromatic, dehydrogenated H0-NEC has a higher tendency for the dealkylation than the hydrogenated or partly hydrogenated Hx-NEC species. This becomes visible from the fact that longer reaction times and further progress of *DoDH* seem to promote the formation of undesired carbazole species. A detailed analysis of the level of carbazole by-products as a function of *DoDH* is shown in Figure 10 and discussed below.

The same byproduct analysis was carried out for the experiment using the carbon-based Pd catalyst. The sum of the molar fraction of carbazole species with this catalyst can be found in table 2.

Table 2: Sum of the molar fractions of all emerging Hx-carbazole by-products in the dehydrogenation reactions of H12-NEC at 200 °C, 180 °C, 160 °C at the pressure levels of 1000 mbar, 500 mbar and 250 mbar after 1 h / 2h / 6 h reaction time.

	***p* = 1000 mbar**	***p* = 500 mbar**	***p* = 250 mbar**
***T* = 200 °C**	0.3 % / 1.0 % / 1.7 %	0.7 % / 1.8 % / 2.8 %	1.4 % / 2.6 % / 3.3 %
***T* = 180 °C**	1.5 % / 1.5 % / 1.3 %	1.3 % / 1.6 % / 3.9 %	1.6 % / 1.9 % / 3.6 %
***T* = 160 °C**	0.9 % / 1.4 % / 0.9 %	1.0 % / 1.2 % / 1.8 %	1.1 % / 1.4 % / 0.5 %

Experimental conditions: $n_{H12\text{-}NEC,0}$ = 0.05 mol, n_{Pd} : $n_{H12\text{-}NEC}$ = 1 : 1000; catalyst: Pd/carbon 5 wt. %.

Again the general trend is visible that C-N cleavage is promoted at higher temperatures and lower total pressures. At 160 °C, it seems that carbazole by-products disappear at longer reaction times. In this context it is noteworthy, that the by-products analysis under these conditions is at the lower end of the detection range of our GC analysis. This may increase the relative error of the quantitative determination. It can, however, not be excluded that formed carbazol species adsorb over time to the carbon support of the catalyst and are thus removed from the analyzed liquid product mixture.

The comparative analysis of the carbazole by-products as a function of catalyst material and *DODH* shown in Figure 10 reveals a couple of interesting aspects: i) the absolute level of carbazole by-product formation and its dependency on *DODH* is in a similar order of magnitude for both catalyst materials and show similar *DODH* dependencies; ii) the by-product formation shows a different profile at 200°C compared to 180 °C. At 200 °C the carbazole by-product formation seems to be more sensitive on the *DoDH* level with strong by-product formation occurring preferentially at high *DODH* levels; iii) the pressure dependency on by-product formation is less clear than expected; this is probably due to a complex interplay of reaction pathways that depend strongly on the absolute aromatics content in the reaction mixture and those that are strictly reaction time dependent. Note, that more reaction time is required to reach a certain *DoDH* in the case of higher total pressure in the dehydrogenation reaction system.

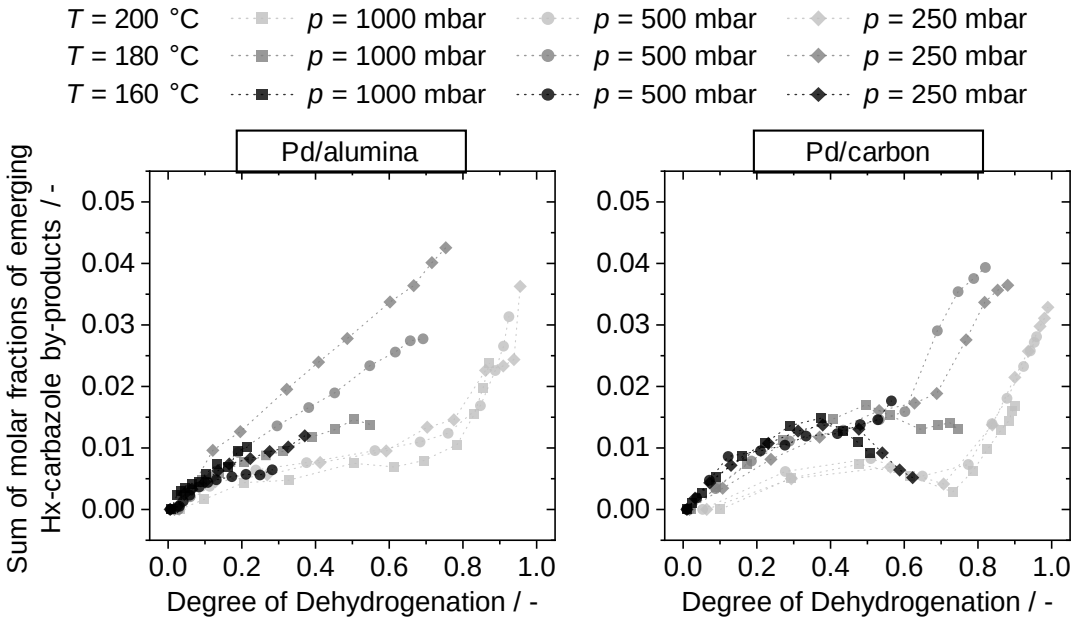

Figure 10: Sum of the molar fractions of all emerging Hx-carbazole by-products in the dehydrogenation reactions of H12-NEC with Pd/alumina (left) and Pd/carbon (right)
Experimental conditions: $n_{\text{H12-NEC,0}}$ = 0.05 mol, n_{Pd} : $n_{\text{H12-NEC}}$ = 1 : 1000.

Conclusion

The LOHC technology can significantly benefit from heat integration between the waste heat of a high temperature PEM fuel cell and the endothermal dehydrogenation reaction. For this purpose, we have targeted in this study lower LOHC dehydrogenation temperatures by operating the hydrogen release from H12-NEC at reduced total pressures. Our results indicate that lowering the reaction pressures down to 250 mbar does indeed accelerate dehydrogenation rates at temperatures down to 160 °C with commercial Pd on alumina and Pd on carbon catalysts in a significant manner. The comparison of these two catalysts reveals that the carbon-based palladium catalyst is more active and more suitable for low temperature dehydrogenation applications. Initial productivities of 0.637 and 0.350 $g(H_2)/(g(Pd) \cdot min)$ were reached with the studied Pd on carbon catalyst at 180 °C and 160°C, respectively, at a total pressure level of 250 mbar. These productivities are well in the suitable range for combined hydrogen release/electrification applications in combination with a HT-PEM fuel cell. Moreover, the fuel cell is able to generate such pressure levels when sucking hydrogen from the release unit during operation. It is well understood that such sucking operation mode of the fuel cell would make some modifications in the set-up necessary, e.g. it would require a purging system for the FC anode chamber to avoid accumulation of inert compounds in the anode chamber. Further research on specially designed fuel cells for sucking operation mode is certainly necessary to enable the implementation of the here-proposed technology in a low-cost and space-optimized efficient manner. It is, however, not expected that a sucking operation mode will lead to a major loss in fuel cell performance as the latter is limited mainly by the cathodic oxygen reduction.

Literature

[1] P.M. Modisha, C.N.M. Ouma, R. Garidzirai, P. Wasserscheid, and D. Bessarabov, *The Prospect of Hydrogen Storage Using Liquid Organic Hydrogen Carriers,* Energy & Fuels, **33**(4), 2778-2796 (2019).

[2] D. Teichmann, W. Arlt, P. Wasserscheid, and R. Freymann, *A future energy supply based on Liquid Organic Hydrogen Carriers (LOHC),* Energy & Environmental Science, **4**(8), 2767-2773 (2011).

[3] D. Teichmann, W. Arlt, and P. Wasserscheid, *Liquid Organic Hydrogen Carriers as an efficient vector for the transport and storage of renewable energy,* International Journal of Hydrogen Energy, **37**(23), 18118-18132 (2012).

[4] A. Bulgarin, H. Jorschick, P. Preuster, A. Bösmann, and P. Wasserscheid, *Purity of hydrogen released from the Liquid Organic Hydrogen Carrier compound perhydro dibenzyltoluene by catalytic dehydrogenation,* International Journal of Hydrogen Energy, **45**(1), 712-720 (2020).

[5] K. Müller, K. Stark, V.N. Emel'yanenko, M.A. Varfolomeev, D.H. Zaitsau, E. Shoifet, C. Schick, S.P. Verevkin, and W. Arlt, *Liquid organic hydrogen carriers: thermophysical and thermochemical studies of benzyl-and dibenzyl-toluene derivatives,* Industrial & Engineering Chemistry Research, **54**(32), 7967-7976 (2015).

[6] P. Runge, C. Sölch, J. Albert, P. Wasserscheid, G. Zöttl, and V. Grimm, *Economic comparison of different electric fuels for energy scenarios in 2035,* Applied Energy, **233**, 1078-1093 (2019).

[7] G.W.H. Scherer and E. Newson, *Analysis of the seasonal energy storage of hydrogen in liquid organic hydrides,* International Journal of Hydrogen Energy, **23**(1), 19-25 (1998).

[8] C.-Y. Wang, *Fundamental Models for Fuel Cell Engineering,* Chemical Reviews, **104**(10), 4727-4766 (2004).

[9] F. Alhumaidan, D. Cresswell, and A. Garforth, *Hydrogen Storage in Liquid Organic Hydride: Producing Hydrogen Catalytically from Methylcyclohexane,* Energy & Fuels, **25**(10), 4217-4234 (2011).

[10] M. Niermann, A. Beckendorff, M. Kaltschmitt, and K. Bonhoff, *Liquid Organic Hydrogen Carrier (LOHC) – Assessment based on chemical and economic properties,* International Journal of Hydrogen Energy, **44**(13), 6631-6654 (2019).

[11] K. Müller, S. Thiele, and P. Wasserscheid, *Evaluations of Concepts for the Integration of Fuel Cells in Liquid Organic Hydrogen Carrier Systems,* Energy & Fuels, **33**(10), 10324-10330 (2019).

[12] Q. Li, D. Aili, H.A. Hjuler, and J.O. Jensen, *High temperature polymer electrolyte membrane fuel cells,* Springer Switzerland, 387-425 (2016).

[13] T. Søndergaard, L.N. Cleemann, H. Becker, D. Aili, T. Steenberg, H.A. Hjuler, L. Seerup, Q. Li, and J.O. Jensen, *Long-term durability of HT-PEM fuel cells based on thermally cross-linked polybenzimidazole,* Journal of Power Sources, **342**, 570-578 (2017)

[14] T.J. Schmidt, *Durability and Degradation in High-Temperature Polymer Electrolyte Fuel Cells*, in *ECS Transactions*. 2006, ECS.

[15] Y. Oono, A. Sounai, and M. Hori, *Prolongation of lifetime of high temperature proton exchange membrane fuel cells,* Journal of Power Sources, **241**, 87-93 (2013).

[16] Y. Oono, A. Sounai, and M. Hori, *Long-term cell degradation mechanism in high-temperature proton exchange membrane fuel cells,* Journal of Power Sources, **210**, 366-373 (2012).

[17] S.S. Araya, F. Zhou, V. Liso, S.L. Sahlin, J.R. Vang, S. Thomas, X. Gao, C. Jeppesen, and S.K. Kær, *A comprehensive review of PBI-based high temperature PEM fuel cells,* International Journal of Hydrogen Energy, **41**(46), 21310-21344 (2016).

[18] P. Preuster, A. Alekseev, and P. Wasserscheid, *Hydrogen Storage Technologies for Future Energy Systems,* Annual Review of Chemical and Biomolecular Engineering, **8**(1), 445-471 (2017).

[19] K. Müller, K. Stark, V.N. Emel'yanenko, M.A. Varfolomeev, D.H. Zaitsau, E. Shoifet, C. Schick, S.P. Verevkin, and W. Arlt, *Liquid Organic Hydrogen Carriers: Thermophysical and Thermochemical Studies of Benzyl- and Dibenzyl-toluene Derivatives,* Industrial & Engineering Chemistry Research, **54**(32), 7967-7976 (2015).

[20] A.C. Cooper, K.M. Campbell, and G.P. Pez. *An integrated hydrogen storage and delivery approach using organic liquid-phase carriers*. in *Proc. 16th World Hydrogen Energy Conference, Lyon, France*. 2006.

[21] J. Von Wild, T. Friedrich, A. Cooper, B. Toseland, G. Muraro, W. TeGrotenhuis, Y. Wang, P. Humble, and A. Karim, *Liquid Organic Hydrogen Carriers (LOHC): An auspicious alternative to conventional hydrogen storage technologies,* Proceedings WHEC, 189-197 (2010).

[22] A. Moores, M. Poyatos, Y. Luo, and R.H. Crabtree, *Catalysed low temperature H 2 release from nitrogen heterocycles,* New Journal of Chemistry, **30**(11), 1675-1678 (2006).

[23] E. Newson, T. Haueter, P. Hottinger, F. Von Roth, G.W.H. Scherer, and T.H. Schucan, *Seasonal storage of hydrogen in stationary systems with liquid organic hydrides,* International Journal of Hydrogen Energy, **23**(10), 905-909 (1998).

[24] M. Geißelbrecht, S. Mrusek, K. Müller, P. Preuster, A. Bösmann, and P. Wasserscheid, *Highly efficient, low-temperature hydrogen release from perhydro-benzyltoluene using reactive distillation,* Energy & Environmental Science, **13**(9), 3119-3128 (2020).

[25] K. Stark, V.N. Emel'yanenko, A.A. Zhabina, M.A. Varfolomeev, S.P. Verevkin, K. Müller, and W. Arlt, *Liquid organic hydrogen carriers: thermophysical and*

thermochemical studies of carbazole partly and fully hydrogenated derivatives, Industrial & Engineering Chemistry Research, **54**(32), 7953-7966 (2015).

[26] I.Y. Choi, B.S. Shin, S.K. Kwak, K.S. Kang, C.W. Yoon, and J.W. Kang, *Thermodynamic efficiencies of hydrogen storage processes using carbazole-based compounds*, International Journal of Hydrogen Energy, **41**(22), 9367-9373 (2016).

[27] B.S. Shin, C.W. Yoon, S.K. Kwak, and J.W. Kang, *Thermodynamic assessment of carbazole-based organic polycyclic compounds for hydrogen storage applications via a computational approach*, International Journal of Hydrogen Energy, **43**(27), 12158-12167 (2018).

[28] R.H. Crabtree, *Hydrogen storage in liquid organic heterocycles*, Energy & Environmental Science, **1**(1), 134-138 (2008).

[29] F. Sotoodeh, B.J.M. Huber, and K.J. Smith, *The effect of the N atom on the dehydrogenation of heterocycles used for hydrogen storage*, Applied Catalysis A: General, **419-420**, 67-72 (2012).

[30] F. Sotoodeh and K.J. Smith, *Kinetics of Hydrogen Uptake and Release from Heteroaromatic Compounds for Hydrogen Storage*, Industrial & Engineering Chemistry Research, **49**(3), 1018-1026 (2010).

[31] K.M. Eblagon, D. Rentsch, O. Friedrichs, A. Remhof, A. Zuettel, A. Ramirez-Cuesta, and S.C. Tsang, *Hydrogenation of 9-ethylcarbazole as a prototype of a liquid hydrogen carrier*, international journal of hydrogen energy, **35**(20), 11609-11621 (2010).

[32] M. Sobota, I. Nikiforidis, M. Amende, B.S. Zanón, T. Staudt, O. Höfert, Y. Lykhach, C. Papp, W. Hieringer, and M. Laurin, *Dehydrogenation of Dodecahydro-N-ethylcarbazole on Pd/Al_2O_3 Model Catalysts*, Chemistry–A European Journal, **17**(41), 11542-11552 (2011).

[33] G.P. Pez, A.R. Scott, A.C. Cooper, and H. Cheng, *Hydrogen storage by reversible hydrogenation of pi-conjugated substrates*. 2006, Google Patents.

[34] N. Brückner, K. Obesser, A. Bösmann, D. Teichmann, W. Arlt, J. Dungs, and P. Wasserscheid, *Evaluation of Industrially applied heat-transfer fluids as liquid organic hydrogen carrier systems*, ChemSusChem, **7**(1), 229-235 (2014).

[35] DOE Technical Targets for Onboard Hydrogen Storage for Light-Duty Vehicles, OFFICE of ENERGY EFFICIENCY & RENEWABLE ENERGY, Last accessed: November 2020.

[36] F. Sotoodeh, L. Zhao, and K.J. Smith, *Kinetics of H2 recovery from dodecahydro-N-ethylcarbazole over a supported Pd catalyst*, Applied Catalysis A: General, **362**(1-2), 155-162 (2009).

[37] M. Amende, S. Schernich, M. Sobota, I. Nikiforidis, W. Hieringer, D. Assenbaum, C. Gleichweit, H.J. Drescher, C. Papp, and H.P. Steinrück, *Dehydrogenation mechanism of liquid organic hydrogen carriers: dodecahydro-N-ethylcarbazole on Pd (111)*, Chemistry–A European Journal, **19**(33), 10854-10865 (2013).

[38] M. Yang, Y. Dong, and H.S. Cheng. *Hydrogenation Kinetics of N-ethylcarbaozle as a heteroaromatic liquid organic hydrogen carrier*. in *Advanced Materials Research*. 2014. Trans Tech Publ.

[39] M.J. Schneider. *Hydrogen storage and distribution via liquid organic carriers*. in *Bridging Renewable Electricity with Transportation Fuels Workshop, Brown Palace Hotel, Denver, CO, August*. 2015.

[40] P. Preuster, C. Papp, and P. Wasserscheid, *Liquid Organic Hydrogen Carriers (LOHCs): Toward a Hydrogen-free Hydrogen Economy*, Accounts of Chemical Research, **50**(1), 74-85 (2017).

[41] C. Gleichweit, M. Amende, S. Schernich, W. Zhao, M.P. Lorenz, O. Höfert, N. Brückner, P. Wasserscheid, J. Libuda, and H.P. Steinrück, *Dehydrogenation of Dodecahydro-N-ethylcarbazole on Pt (111),* ChemSusChem, **6**(6), 974-977 (2013).

[42] M. Yang, Y. Dong, S. Fei, H. Ke, and H. Cheng, *A comparative study of catalytic dehydrogenation of perhydro-N-ethylcarbazole over noble metal catalysts*, International journal of hydrogen energy, **39**(33), 18976-18983 (2014).

[43] W. Peters, A. Seidel, S. Herzog, A. Bösmann, W. Schwieger, and P. Wasserscheid, *Macrokinetic effects in perhydro-N-ethylcarbazole dehydrogenation and H 2 productivity optimization by using egg-shell catalysts*, Energy & Environmental Science, **8**(10), 3013-3021 (2015).

[44] F. Sotoodeh and K.J. Smith, *Structure sensitivity of dodecahydro-N-ethylcarbazole dehydrogenation over Pd catalysts*, Journal of catalysis, **279**(1), 36-47 (2011).

[45] F. Sotoodeh, B.J.M. Huber, and K.J. Smith, *Dehydrogenation kinetics and catalysis of organic heteroaromatics for hydrogen storage*, International Journal of Hydrogen Energy, **37**(3), 2715-2722 (2012).

[46] Z. Jiang, Q. Pan, J. Xu, and T. Fang, *Current situation and prospect of hydrogen storage technology with new organic liquid*, International Journal of Hydrogen Energy, **39**(30), 17442-17451 (2014).

Supporting information

Dehydrogenation of Perhydro-N-ethylcarbazole Under Reduced Total Pressure

Stephan Kiermaier[a], Daniel Lehmann[a], Andreas Bösmann[a], Peter Wasserscheid[a,b]*

[a] Lehrstuhl für Chemische Reaktionstechnik, Friedrich-Alexander-Universität Erlangen-Nürnberg (FAU), Egerlandstr. 3, D-91058,

[b] Helmholtz-Institute Erlangen-Nürnberg for Renewable Energies, IEK-11, Forschungszentrum Jülich, Nägelsbachstraße 59, 91058 Erlangen, Germany

* Corresponding author. E-mail: peter.wasserscheid@fau.de

A Detailed composition of a typical product mixture from H0-NEC hydrogenation

Table S1: Degree of hydrogenation (DoH), molar fractions of the Hx-NEC intermediates and by-products of a typical product mixture obtained after H0-NEC hydrogenation

DoH / %	> 99
Molar fraction H12-NEC / %	> 98
Molar fraction of H8-NEC / %	< 2
Molar fraction of carbazole-based by-products / %	< 1

Experimental conditions: T = 160 °C, p_{H_2} = 40 bar $n_{H0\text{-}NEC}$ = 0.75 mol, $n_{Ru} : n_{H0\text{-}NEC}$ = 1 : 1000, $n_{Pd} : n_{H0\text{-}NEC}$ = 1 : 2000; catalyst: Ru/alumina 5 wt. % and Pd/alumina 5 wt. %

For further information on the GC/GC-MS retention times and identification of the Hx-NEC and Hx-C components, the interested reader can contact the author Stephan Kiermaier (stephan,kiermaier@fau.de).

B Physicochemical properties of the dehydrogenation catalyst

Table S2: Physicochemical properties of the catalysts used in the dehydrogenation reactions of H12-N-ethylcarbazole.

	Pd/alumina Sigma Aldrich Batch # : 10221PE	Pd/carbon Sigma Aldrich Lot # : MKBS9242V
BET surface[a] / $m^2 \cdot g^{-1}$	120	1070
Pd-content[b] / %	5.0	5.0
Dispersion[c] / %	22.3	23.7
Pd particle diameter[a] / nm	5.0	4.7
Average pore diameter / nm	9.0	3.6

[a] Determined via N_2 physisorption
[b] From certificate of analysis supplied by Sigma Aldrich
[c] Determined via CO chemisorption

The Ru/alumina catalyst that was used together with the above mentioned Pd/alumina catalyst for the hydrogenation of H0-NEC was from Alfa Aesar (5 wt. %; Lot #: X12E020)

C Rate constants *k* of the H12-NEC consumption

The rate constants *k* were estimated via a first-order kinetic model that was fitted to the consumption of perhydro-N-ethylcarbazole (H12-NEC) for the experimental data obtained during the first 2 h reaction time. The respective *k*-values are shown in Figure S1 for the Pd/alumina catalyst.

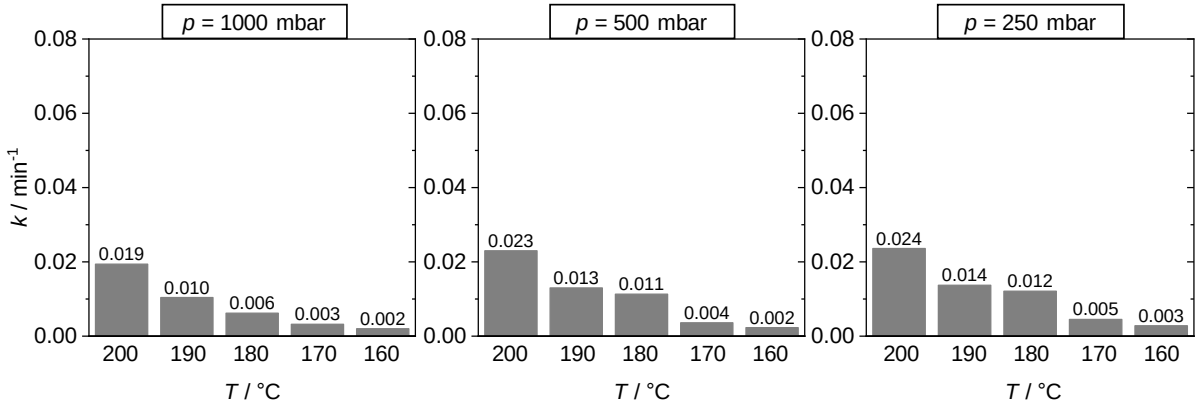

Figure S1: Rate constants *k* of the H12-NEC consumption during the dehydrogenation reactions of H12-NEC at the temperature levels of 200 °C, 190 °C, 180 °C, 170 °C and 160 °C at a pressure of 1000 mbar (left), 500 mbar (middle) and 250 mbar (right) after 2 h; experimental conditions: $n_{\text{H12-NEC,0}}$ = 0.05 mol, n_{Pd} : $n_{\text{H12-NEC}}$ = 1 : 1000; catalyst: Pd/alumina 5 wt. %.

The rate constants *k* that were determined during the dehydrogenations reactions with the Pd/carbon catalyst can be found in Figure S2.

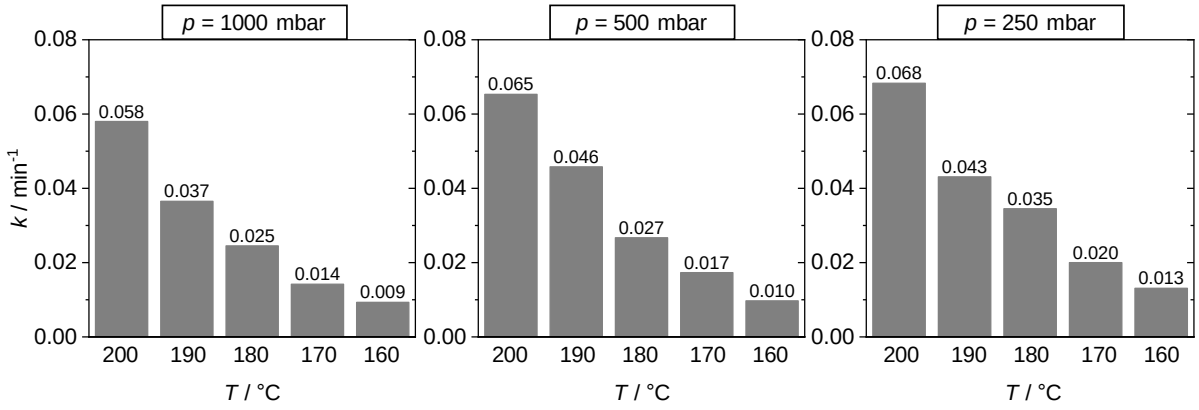

Figure S2: Rate constants *k* of the H12-NEC consumption during the dehydrogenation reactions of H12-NEC at the temperature levels of 200 °C, 190 °C, 180 °C, 170 °C and 160 °C at a pressure of 1000 mbar (left), 500 mbar (middle) and 250 mbar (right) after 2 h; experimental conditions: $n_{\text{H12-NEC,0}}$ = 0.05 mol, n_{Pd} : $n_{\text{H12-NEC}}$ = 1 : 1000; catalyst: Pd/carbon 5 wt. %.

D Activation energies of the first step of H12-NEC dehydrogenation

The activation energies were determined from an Arrhenius plot of the above mentioned rate constants *k* of the H12-NEC consumption reactions.

Table S3: Activation energies of the first step of the H12-NEC dehydrogenation reaction (consumption of H12-NEC).

	Pd/alumina	Pd/carbon
p = 1000 mbar	97.4 kJ / mol	78.5 kJ / mol
p = 500 mbar	100.6 kJ / mol	81.7 kJ / mol
p = 250 mbar	91.9 kJ / mol	69.4 kJ / mol

Experimental conditions: $n_{H12\text{-}NEC,0}$ = 0.05 mol, n_{Pd} : $n_{H12\text{-}NEC}$ = 1 : 1000.

E Schematic of the reactor setup

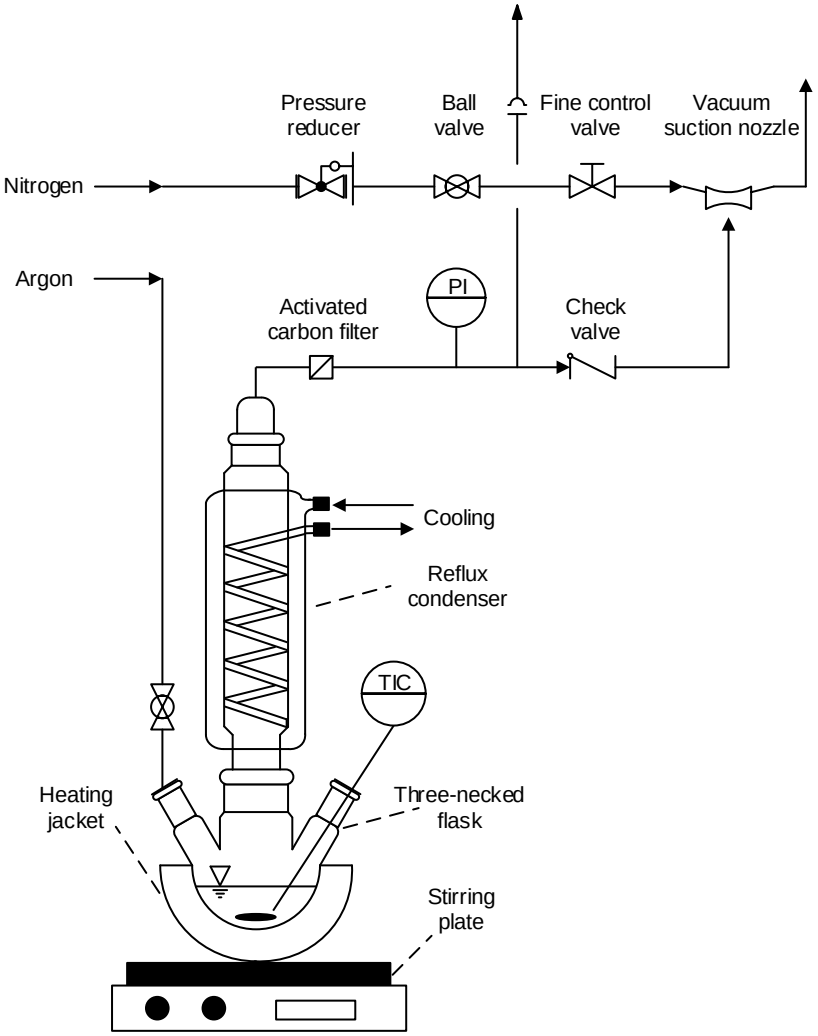

Figure S3: Schematic of the reactor setup for the dehydrogenation of perhydro-N-ethylcarbazol under reduced total pressure.